International Journal of Science and Research (IJSR)
ISSN (Online): 2319-7064
Index Copernicus Value (2016): 79.57 | Impact Factor (2015): 6.391

Quantum Chemical Calculations and Experimental Studies on 2(2, 3-dimethylphenyl) Amino Benzoic Acid

R. Padmavathi[1], S. Gunasekaran[2], B. Rajamannan[3], G. R. Ramkumar[4], G. Sankari[5], S. Muthu[6]

[1]Department of Physics, Meenakshi Sundararajan Engineering College, Kodambakkam, Chennai-600024, TN, India

[2]Sophisticated Analytical Instrumentation Facility, St. Peter's institute of Higher Education and Research, St. Peter's University, Avadi, Chennai-600054, TN, India

[3]Engineering Physics, FEAT Annamalai University, Annamalai Nagar- 608002, and Chidambaram, TN, India

[4]Department of Physics, C. Kandaswaminaidu College for Men, Anna Nagar East, Chenna-600102, TN, India

[5]Department of Physics, Meenakshi College for Womens, Kodambakkam, Chennai-600024, TN, India

[6]Department of physics, Govt. Thirumagal Mills College, Gudiyatham-632602 Vellore-TN, India

Abstract: ***The Fourier transformation Infrared (FTIR) and FT-Raman (FTR) spectra of 2-[(2, 3-dimethylphenyl) amino benzoic acid (MFA) have been recorded in the regions 4000-450cm^{-1}and 4000-50cm^{-1}respectively. Utilizing the observed FTIR and FT-Raman data, a complete vibrational assignment and analysis of the fundamental modes of MFA have been carried out. The optimum molecular geometry, infrared intensities have been calculated by density functional theory (DFT/B3LYP) method with 6-31G (d, p), 6-31++G(d, p) basis sets. The complete vibrational assignments were performed on the basis of the potential energy distribution (PED) of the Vibrational modes calculated using Vibrational Energy Distribution Analysis (VEDA 4) program. The thermodynamic properties like Entropy, Enthalpy, Specific Heat Capacity and Zero vibrational energy have been calculated. HOMO-LUMO energy gap and Fukui functions, local softness and local electrophilicity has been calculated. Besides, molecular Electrostatic potential (MEP) was investigated using theoretical calculations.***

Keywords: MFA, FTIR, FT –Raman, HOMO-LUMO, Mullikan atomic charges, MEP, Fukui function

1. Introduction

Mefenamic acid (Ponstan/MFA) is a member of anthranilic acid derivatives class of non-steroidal anti-inflammatory drug (NSAID). Its IUPAC name is 2-[(2, 3-dimethylphenyl) amino benzoic acid is shown in fig [1].Its molecular Mass is 241.285g/mol .MFA is to be kept away from heat, moisture, light and the reach of children and pets. Symptoms of overdose may include severe stomach pain, coffee ground-like vomit, dark stool, ringing in the ears, and change in amount of urine, unusually fast or slow heartbeat and muscle weakness. Anti-inflammatory painkillers are used to treat arthritis, sprains, painful periods, headaches, dental pain and other painful conditions. Similar to other NSAIDs, MFA is used for the treatment of mild to moderate pain from various conditions. It is also used to decrease pain and blood loss from menstrual periods. Mefenamic acid inhibits prostaglandin syntheses. The mechanism of action of Mefenamic acid is similar to Cyclooxygenase inhibitor. MFA is white to off-white crystalline powder sparingly soluble in ether, Chloroform. In 1997 Jilani et al., [1] have synthesized several hydroxyethyl esters of diclofenac andmefenamic acid and studied their stability in HCl, Buffer pH 7.4 and human plasma. Their study revealed that mefenamic acid prodrugs were much more stable than their corresponding diclofenac prodrugs .A.R.Chabukswar et al., [2] tried simultaneous determination of MFA and ethamsylate by area under curve spectrometric method. New investigation results [3], Quantitative evaluation of mefenamic acid polymorphs by terahertz-chemometrics, are detailed in a study published in journal of pharmocetical Sciences. Site Kholijah Abdul Mudalip et al., [4] investigate the molecular recognition of the polymorphism of mefenamic acid form I crystals in ethanol has been successfully revealed through molecular dynamics simulation. The results from FTIR analysis confirmed the existence of hydrogen bonds in mefenamic acid/ethanol solution that lead to the nucleation of mefenamic acid form I crystals. Liang Fang et.al., [5] investigated physiochemical and crystallographic characterization of MF complex's with alkanol amaines.The preparation of mefenamic acid (MH) –(alkanolamine, Triethanolamine) complexes was attempted to increase the transdermal flux of MH, Jerry et al., [6] obtain MFA seed crystals of few millimeters in size by slow evaporation method and studied the crystal structure using X-ray photoelectron Spectroscopy (XPS), using a finite dilution Inverse gas chromatography (FD-IGC) approaches. Serap cesur et al., [7] investigate, MFA is crystallized in ethyl acetate solvent in an isothermal batch crystallize with seed crystals. MFA has some negative properties such as a high hydrophobicity with a propensity to stick to surfaces and possess great problems during granulation and tableting. Crystallization kinetics was investigated for MFA. Vanessa et al., [8] investigate spectroscopic structural and morphological characterization of MFA polymorph, known as form I and II. Polymorph I was obtained by recrystallization in ethanol, while form –II was reached by heating from I up to 175 deg, to promote the solid phase

transition. Experimental and theoretical vibrational band assignments performed considering the presence of centrosymmetric dimers. Besides band shifts in the 3345-3310cm^{-1}, range important vibrational modes to distinguish the polymorphs are related to out- of-phase. Mudit Dixitad partha sarathi K Kulkarani et.al., [9], was tried to improve the solubility and dissolution rate of mefenamic acid by preparing crystals by freeze drying using THF, Isopropyl acetate and water as solvents system to enhance solubility and dissolution rate. The prepared crystals containing mf were evaluated for in vitro dissolution & solubility. The prepared formulations were characterized by scanning electron microscopy, differential scanning calorimeter, X-ray diffraction and Fourier transform infrared spectroscopy. Literature survey reveals that to the best of our knowledge no DFT/B3LYP with 6-31G (d, p)/, 6-31++G(d, p) and RHF/6-311G(d, p) basis sets calculations of MFA have been reported so for. Therefore an attempt has been made in present study about the detailed theoretical DFT and experimental (FTIR, FT_RAMAN) spectral investigation of MFA. The results of the theoretical and spectroscopic studies are reported here in.

2. Experimental

FTIR-ATR spectrum of MFA was carried out at Sophisticated Analytical Instrumentation facility (SAIF-SPU), St. Peter's University, Avadi, Chennai-600 054/India using PerkinElmer spectrum-Two recorded in the regions 4000-450cm^{-1}.FTIR Spectrophotometer with attenuated Total Reflectance accessory having highly reliable and single bounce 2mm cross diamond as its Internal Reflectance Element (IRE). FT-Raman spectrum was recorded using 1064 nm line Nd: YAG laser as excitation wavelength in the region 4000-50 cm^{-1} using Bruker RFS 27 spectrometer with 8 scans at a resolution of 2cm^{-1}. The UV–Visible spectral measurements were recorded in the range 200-900nm using a varian Cary 5E-UV-NIR Spectrometer. FT-Raman and UV-Vis spectral measurements were carried out at Sophisticated Analytical Instrument Facility, IIT Madras, India.

3. Computational Details

To provide complete information regarding the structural characteristics and fundamental vibrational modes of MFA, the restricted Hartee-Fock and DFT-B3LYP correlation functional calculations have been carried out. The calculations of geometrical parameters in the ground state were performed using Gaussian 09[10] Programs, invoking gradient geometry optimization [11] on Intel core i3/2.93 GHZ processor. DFT calculations were performed using Becker's three-parameter [12, 13] hybrid model using Lee-yang-Parr (B3LYP) [14] correlation functional method. The computations were performed at RHF, B3LYP, 6-31G(d, p), 6-31++G(d, p) basis sets [15, 16] have been utilized for the computation of molecular structure optimization, geometrical parameters, vibrational scaled wave numbers of the normal modes, IR intensities, atomic charges and thermodynamic parameters of the title compound. The complete assignments were performed on the basis of the potential Energy Distribution (PED) of the vibrational modes, calculated using vibrational Energy Distribution Analysis (VEDA) 4 program

4. Results and Discussion

4.1 Molecular geometry

The optimized molecular structure and atomic numbering of 2(2, 3-dimethylphenyl) amino benzoic acid is shown in Fig.1.The molecule MFA as shown in Fig. 1 has 33 atoms with 93 normal modes of vibration active in both IR and Raman. It belongs to C_1 point group symmetry. Table 1 presents the optimized values obtained for bond lengths and bond angles along with the experimental values. The various bond lengths and bond angles are found to be almost same at B3LYP/6-31G (d, p), 6-31++G(d, p) and RHF/6-311G(d, p) methods. The Bond length between C2-C3 & C6-C7 in B3LYP/6-31G (d, p), 6-31++G (d, p) and RHF/6-311G(d, p) found to be 1.42°, 1.42°, and 1.337° respectively which are in good agreement with the experiment value of 1.419°& 1.4250° respectively. Similarly bond length between C11-C12-C13 & C12- C13-C14 in B3LYP/6-31G (d, p), 6-31++G(d, p) and RHF/6-31++G(d, p) methods are 120°, 120° and119.99° which are in good agreement with experiment value of 120.64°&120.24° The Dihedral angle between H20-C5-C6-C7 by B3LYP/6-31G (d, p), 6-31++G(d, p) and RHF/6-31++G(d, p) methods are found to be 179.42°, 179.42° and 180 which are in good agreement with experimental value of 180 ° respectively. The calculated geometrical parameters can be used to determine other parameters of MFA.

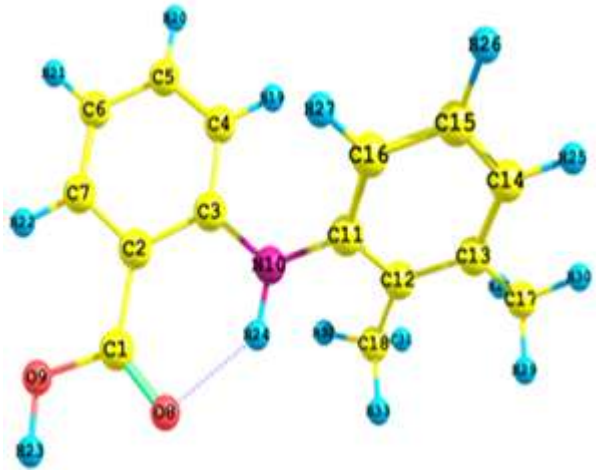

Figure 1: Optimized molecular structure and atomic numbering of2 (2, 3-dimethylphenyl) Amino benzoic acid

4.2 Vibrational analysis

The observed and calculated frequencies using B3LYP method using the basis sets 6-31++G (d, p), 6-31G(d.p) and IR intensities and Vibrational assignments are summarized in Table 2. The FTIR-ATR and FT-Raman spectra of MFA along with experimental and theoretical spectrum are shown in Fig.2 and Fig.3 respectively and the description of band assignments is as follows.

4.2.1 N-H Vibrations

N-H stretching frequencies corresponding to the symmetrical and asymmetrical NH stretching vibrations for

dilute solutions occur near 3520cm^{-1} to 3480cm^{-1}.In the spectra of solid samples are observed near 3350cm^{-1} to 3180cm^{-1} because of hydrogen bonding [17].In the present investigation N-H stretching vibrations are observed at 3310 and 3311cm^{-1} in FTIR and FT-Raman respectively. The theoretically computed values are 3371cm^{-1} and 3381cm^{-1} by B3LYP method with 6-31G(d, p) and 6-31++G(d, p) basis set respectively.

4.2.2 C-C, C-C-C and C-C-C-C Vibrations

The C-C aromatic stretching vibrations give rise to characteristic bands in the both the observed FTIR and FT-Raman spectra covering the spectral region range from 1600-1400cm^{-1} [18].The C-C stretching vibrations are observed at 1648, 1595, 1575, 1503, cm^{-1} in FTIR and 1624, 1602, 1512 cm^{-1} in FT-Raman Spectra respectively. The corresponding theoretical calculated wave numbers are 1706, 1615, 1601, 1588, 1522cm^{-1} and 1681, 1605, 1593, 1578, 1512cm^{-1} by B3LYP methods with 6-31G (d, p) and 6-31++G(d, p) basis set respectively.

The C-C-C bending Vibrations are observed at 1039, 754, 550, 504, 474 cm^{-1} in FTIR and 1040, 743, 505, 475, 320, 283, 247cm^{-1} in FT-Raman Spectra .The corresponding theoretically computed values are 1039, 758, 607, 568, 499, 486, 460, 316, 291, 241cm^{-1}.

4.2.3 O-H Vibrations

The O-H group vibrations are likely to be the most sensitive to the environment, so they show pronounced shifts in the spectra of the hydrogen bonded species. The O-H stretching vibrations are usually observed in the region 3500cm^{-1} [19].The theoretically calculated wave numbers are 3656 and 3657cm^{-1} by B3LYP methods with 6-31G (d, p) and 6-31++G(d, p) basis set respectively and O-H stretching vibrations with PED contribution of 100%. Arivazhagan et al [20] have also assigned B3LYP value 3628 cm^{-1} to O-H stretching.

4.2.4 C-H Vibrations

The C-H stretching vibrations occur above 3000cm^{-1} and are typically exhibited as weak to moderate bands [21].C-H stretching is typically exhibited as a multiplicity of weak to moderate bands, compared with the aliphatic C-H stretching. In our present work 3158, 3147, 3008, 2975, 2950cm $^{-1}$in FTIR and 3072, 2951, 2915cm^{-1} in FT-Raman respectively. The theoretically computed values are 3134, 3132, 3116, 3111, 3098, 3088, 3082, 3047, 3032, 3009, 2995, 2944, 2941cm^{-1}and3133, 3128, 3113, 3111, 3097, 3088, 3081, 3041, 3026, 3006, 2991, 2941, 2937cm^{-1}by B3LYP methods with 6-31G (d, p) and 6-31++G(d, p) basis set respectively. As indicated by PED these modes involve maximum contribution of about 93% suggesting that they are due to pure stretching modes. Arivazhagan et al [22] have also observed C-H stretching at 3000, 2983cm^{-1} in FT-Raman Spectra. Ramkumar et al [23] have reported C-H stretching at 3167, 2933 cm^{-1} in FTIR and at 2941cm^{-1} in FT-Raman Spectra.

4.3 HOMO-LUMO calculation

The most important orbitals in molecules are the frontier molecular orbitals, called highest occupied molecular orbital (HOMO) and lowest unoccupied molecular orbital (LUMO), the main orbitals take part in chemical stability [24]. The HOMO energy characterizes the ability of electron to give or it is the orbital that acts as an electron donor, and LUMO energy characterizes the ability of electron to accept or acts as an electron deficient and hence most subject to nucleophilic attack and the gap between HOMO and LUMO explains the eventual charge transfer interactions taking place within the compound. This influences the biological activity of the molecule. When the energy gap is small the compound will be easily excited. The low values of frontier orbital gap in MFA make it more reactive and less stable. The electron transition absorption corresponds to the transition from the ground to the first excited state and is mainly described by an electron excitation from the HOMO to LUMO energies calculated by B3LYP/6-31G(d, p).HOMO-LUMO energy gap within the molecule are shown in Fig. 4 and calculated energies as follows .

HOMO energy E= -5.60695018 ev
LUMO energy E = -1.60140266 ev
HOMO-LUMO Energy Gap = 4.00554752 ev

4.4 Molecular Electrostatic Potential

The electrostatic potential V (r) that is created in the space around a molecule by its Nuclei and electrons is a very useful property for analyzing and predicting

LUMO (Excited state)

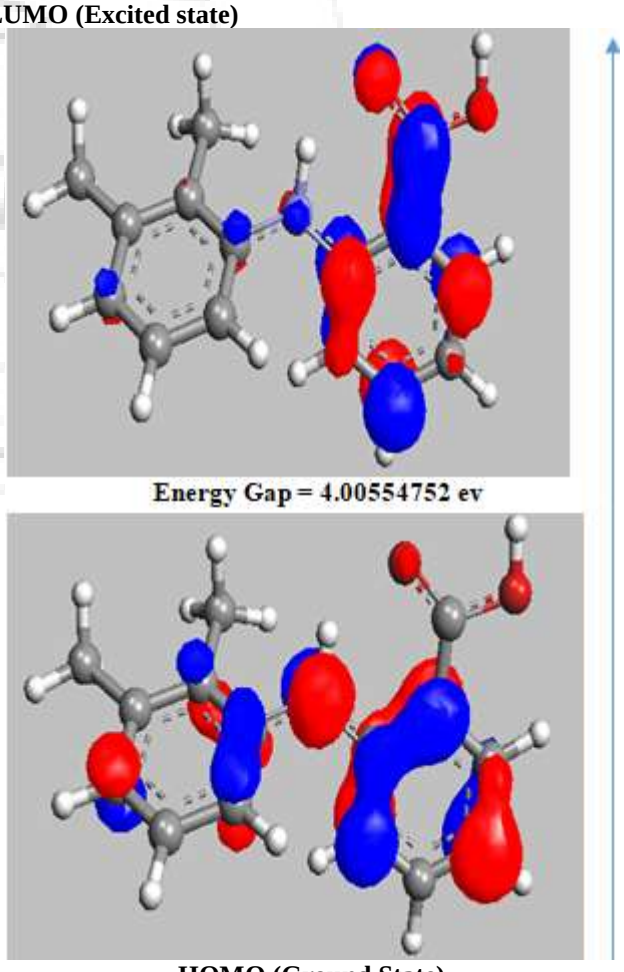

HOMO (Ground State)

Figure 4: 3D plots of HOMO and LUMO B3LYP/6-31G (d, p)

Table 1: Experimental values and theoretically optimized geometrical parameters of MFA obtained by RHF/6-311 G(d, p), B3LYP/6-31G(d, p), 6-31++G(d, p)

S NO	Structural parameter	B3LYP6-31G(d, p)	B3LYP6-31++G(d, p)	RHF/6-311G(d, p)	Expt
1	C1-C2	1.517	1.517	1.351	1.4389 (16)
2	C1-O8	1.208	1.208	1.2079	1.3696(16)
3	C1-O9	1.338	1.338	1.3381	1.3206 (14)
4	C2-C3	1.42	1.42	1.337	1.4199 (16)
5	C2-C7	1.42	1.42	1.3369	1.4407 (16)
6	C3-C4	1.42	1.42	1.337	1.3872 (17)
7	C3-N10	1.462	1.462	1.266	1.4725 (16
8	C4-C5	1.42	1.42	1.337	1.3872 (17)
9	C4-H19	1.1	1.1	1.1	0.95
10	C5-C6	1.42	1.42	1.337	1.3771 (17)
11	C5-H20	1.1	1.1	1.1	0.95
12	C6-C7	1.42	1.42	1.337	1.4250 (17)
13	C6-H21	1.1	1.1	1.1	0.95
14	C7-H22	1.1	1.1	1.1001	0.95
15	O9-H23	0.972	0.972	0.972	0.82
16	N10-C11	1.462	1.462	1.266	
17	N10-H24	1.05	1.05	1.05	
18	C11-C12	1.42	1.42	1.337	1.406 (2)
19	C11-C16	1.42	1.42	1.337	1.406 (2)
20	C12-C13	1.42	1.42	1.3369	1.394 (2)
21	C12-C18	1.497	1.497	1.497	
22	C13-C14	1.42	1.42	1.337	1.390 (3)
23	C13-C17	1.497	1.497	1.4971	
24	C14-C15	1.419	1.419	1.3369	
25	C14-H25	1.1	1.1	1.1001	0.95
26	C15-C16	1.42	1.42	1.1	0 .3898 (19)
27	C15-H26	1.1	1.1	1.1	0.95
28	C16-H27	1.1	1.1	1.1	0.95
29	C17-H28	1.113	1.113	1.113	0.99
30	C17-H29	1.113	1.113	1.113	0.99
31	C17-H30	1.113	1.113	1.113	0.99
32	C18-H31	1.113	1.113	1.113	0.99
33	C18-H32	1.113	1.113	1.113	0.99
34	C18-H33	1.113	1.113	1.113	0.99
	Bond angle				
35	C2-C1-O8	119.8	119.8	120.001	119.65(11)
36	C2-C1-O9	121.2	121.2	119.999	121.21(10)
37	O8-C1-O9	118.8	118.8	120	
38	C1-C2-C3	119.9	119.9	120	120.40(10)
39	C1-C2-C7	119.9	119.9	120.002	
40	C3-C2-C7	120	120	119.999	119.64(10)
42	C2-C3-C4	120	120	120	120.59(11)
43	C2-C3-N10	119.9	119.9	120.001	122.58
44	C4-C3-N10	119.9	119.9	120	122.58
45	C3-C4-C5	120	120	120	119.21(11)
46	H28-C17-H30	109	109	109.461	108
47	H29-C17-H30	110	110	109.522	108
48	C12-C18-H31	110	110	109.498	109
49	C12-C18-H32	110	110	109.444	109
50	C12-C18-H33	110	110	109.461	109
51	H31-C18-H32	110	110	109.437	108
52	H31-C18-H33	109	109	109.463	108
53	C3-C4-H19	119.9	119.9	120.001	119
54	C5-C4-H19	119.9	119.9	120	119
55	C4-C5-C6	120	120	120.001	121.21(11)
56	C4-C5-H20	119.9	119.9	120	119
57	C6-C5-H20	119.9	119.9	120	119
58	C5-C6-C7	120	120	119.995	119.5(10)
59	C5-C6-H21	119.9	119.9	120	119
60	C7-C6-H21	119.9	119.9	120.005	119
61	C2-C7-C6	120	120	120.006	119.95
62	C2-C7-H22	119.9	119.9	120	119
63	C6-C7-H22	119.9	119.9	119.994	119
64	C1-O9-H23	106.1	106.1	119.999	109

65	C3-N10-C11	124	124	120.001	123.74(10)
66	C3-N10-H24	117.9	117.9	120	118
67	C11-N10-H24	117.9	117.9	120	118
68	N10-C11-C12	120	120	120.001	111.47(13)
69	N10-C11-C16	119.9	119.9	120	122.58(11)
70	C12-C11-C16	119.9	119.9	120	9
71	C11-C12-C13	120	120	119.999	120.64(15)
72	C11-C12-C18	119.9	119.9	120	120.53(14)
73	C13-C12-C18	119.9	119.9	120.002	118.18(12)
74	C12-C13-C14	120	120	120.002	120.24(17)
75	C12-C13-C17	119.9	119.9	120	119.97(15)
76	C14-C13-C17	119.9	119.9	119.999	119.87(15)
77	C13-C14-C15	120	120	120.002	119.97(15)
78	C13-C14-H25	119.9	119.9	119.998	120
79	C15-C14-H25	119.9	119.9	120	120
80	C14-C15-C16	120	120	119.999	119.87(15)
81	C14-C15-H26	119.9	119.9	120.002	120
82	C16-C15-H26	119.9	119.9	120	120
83	C11-C16-C15	120	120	120	121.08(15)
84	C11-C16-H27	119.9	119.9	120.001	119
85	C15-C16-H27	119.9	119.9	120	119
86	C13-C17-H29	110	110	109.439	109
87	C13-C17-H30	110	110	109.461	109
88	H28-C17-H29	109	109	109.443	108
89	Dihedral angle(◦)				
90	O8-C1-C2-C3	0.5653	0.5653	180	179.54(14)
91	O8-C1-C2-C7	_178.86	_178.86	0	1.3(2)
92	O9-C1-C2-C3	180	180	0	179.78(16)
93	C2-C1-O9-H23	180	180	180	
94	O8-C1-O9-H23	_0.5599	_0.5599	0	
95	C1-C2-C3-C4	_179.42	_179.42	180	
96	C1-C2-C3-N10	1.1458	1.1458	0	
97	C7-C2-C3-C4	0	0	0	0.1(3)
98	C7-C2-C3-N10	_179.42	_179.42	180	
99	C14-C15-C16-H27	_179.42	_179.42	119.999	
100	H26-C15-C16-C11	179.42	179.42	180	
101	H26-C15-C16-H27	0	0	0	
102	C3-C2-C7-H22	179.42	179.42	180	
103	C2-C3-C4-C5	0	0	180	0.7
104	C2-C3-C4-H19	_179.42	_179.42	180	
105	N10-C3-C4-C5	179.42	179.42	180	
106	N10-C3-C4-H19	0	0	0	
107	C2-C3-N10-C11	120	120	180	
108	C2-C3-N10-H24	_59.46	_59.46	0	
109	C4-C3-N10-C11	_59.42	_59.42	0	
110	C4-C3-N10-H24	121.11	121.11	180	
111	C3-C4-C5-C6	0	0	0	
112	C3-C4-C5-H20	_179.42	_179.42	180	
113	H19-C4-C5-C6	179.42	179.42	180	
114	H19-C4-C5-H20	0	0	0	
115	C4-C5-C6-C7	0	0	0	
116	H20-C5-C6-C7	179.42	179.42	180	
117	H20-C5-C6-H21	0	0	0	
118	C5-C6-C7-C2	0	0	0	
119	C5-C6-C7-H22	_179.42	_179.42	180	
120	C3-N10-C11-C12	_120.0	_120.0	180	
121	C3-N10-C11-C16	59.4	59.4	0	
122	H24-N10-C11-C12	59.4	59.4	0	
123	H24-N10-C11-C16	_121.11	_121.11	180	
124	N10-C11-C12-C13	179.42	179.42	180	177.35(15)
125	C1-C2-C7-C6	179.42	179.42	180	
126	C1-C2-C7-H22	_1.1459	_1.1459	0	
127	C3-C2-C7-C6	0	0	0	

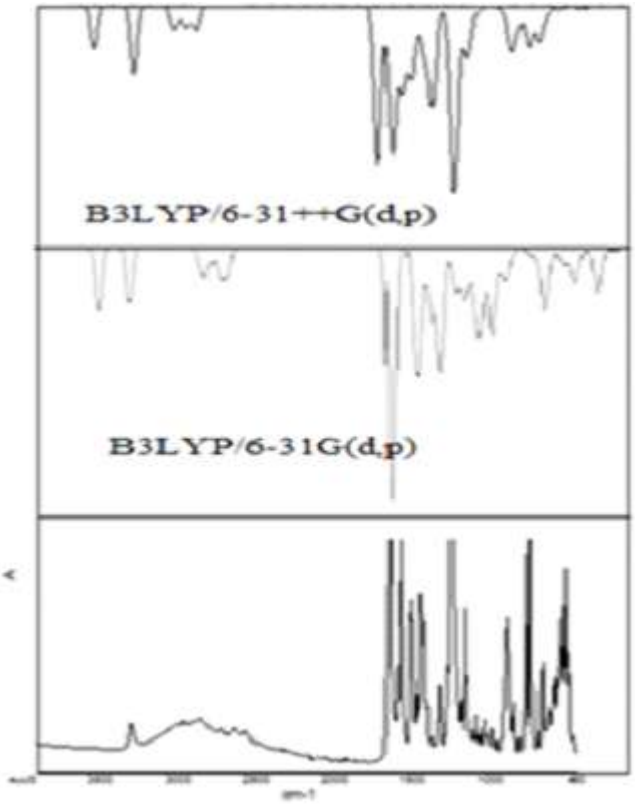

Figure 2: FTIR-ATR Spectrum of MFA

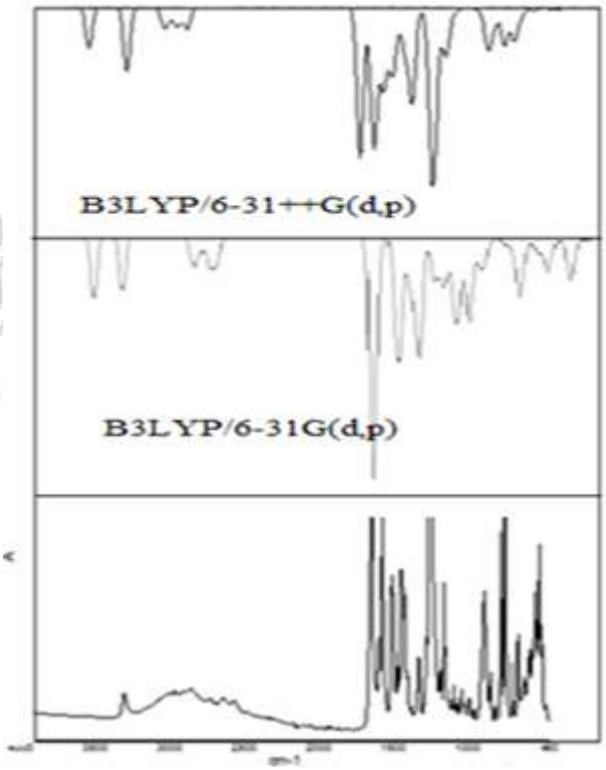

Figure 3: FT-Raman Spectrum of MFA

Table 2: The observed and calculated frequencies of MFA using B3LYP/6-31G(d, p) and B3LYP/6-31++G(d, p) methods

Experimental wave numbers(cm^{-1})		Theoretical Wavenumbers (cm^{-1})				Vibrational assignments
		B3LYP/6-31G(d, p)		B3LYP/6-31++G(d, p)		
FTIR	FT-Raman	scaled Frequency	Intensity	scaled Frequency	Intensity	
		3656	90.53	3657	111.73	001Hν
3310	3311	3371	184.04	3381	176.86	νNH100
3158		3134	3.71	3133	4.61	νCH(90)
3147	3072	3132	7.32	3128	4.1103	νCH(95)
3008		3116	8.04	3113	7.3869	νCH(84)
2975		3111	14.79	3111	13.3248	νCH(84)
2950		3098	30.53	3097	26.8262	νCH(87)
2912		3088	9.53	3088	8.1536	νCH(97)
2860	2951	3082	5.4	3081	9.9427	νCH(68)
2732	2915	3047	9.31	3041	9.9427	νCH(93)
2644		3032	21.4301	3026	23.3574	νCH(91)
2570		3009	16.2	3006	15.8324	νCH(100)
2495	2729	2995	22.3	2991	19.824	νCH(99)
2494	2569	2944	34.05	2941	37.3267	νCH(61)
		2941	19.93	2937	21.879	νCH(49)
1648	1624	1706	312.52	1681	417.8673	νCC(83)+bHCC(10)
		1615	84.89	1605	71.195	νCC(56)
1595	1602	1601	38.39	1593	25.4013	νCC(22)+ bccc(10)
1575		1588	89.32	1578	40.2985	νCC(11)+ bHNC(12)
1510	1581	1585	245.96	1574	298.4051	νOC(37)+bHOC(10)
1503	1512	1522	230.21	1512	215.1568	νCC(13)+bHCC(11)+bHNC(25)
		1478	52.64	1471	53.8304	bHCC(16)+ b HCC(12)
1471		1471	11.61	1464	9.0539	b HCC(28)
		1467	4.8	1458	4.5301	b HCH(88)
		1460	1.92	1451	4.3292	b HCC(29)
		1451	76.03	1443	74.8166	b HCH(35)
1446	1446	1447	28.32	1439	26.5223	b HCH(39)
1425		1445	38.72	1438	32.6646	b HNC(22)
1407	1403	1418	40.19	1412	36.9776	b HCH(24)
		1390	0.9	1383	2.3335	b HCH(63)
		1381	1.53	1374	0.6729	b HCH(26)
1379	1384	1371	116.64	1355	107.8192	νOC(11)+νCC(11)+b HCC(12)
1329	1333	1323	68.76	1317	54.4741	νNC(17)+b HOC(20)+ b HCC(13)
		1307	165.65	1298	178.8218	νNC(24)
		1298	2.88	1292	43.5666	b HCC(49)
1278	1278	1274	1.87	1267	0.7698	b HCC(15)+ν NX (11)
1256		1243	0.8	1238	0.8439	νCC(13)+b HOC(31)
		1223	7.57	1218	8.7199	νCC(12)+νOC(10)+b HCC(47)
1185	1186	1173	76.59	1170	9.9101	νCC(35)+b HCC(23)
		1170	216.36	1163	173.6517	ν CC(31)+b HCC(17)
1162	1161	1163	3.2	1158	7.4885	ν CC (31)b HCC(31)
		1155	168.03	1150	228.115	ν CC (32)+b HCC (12)
1095	1094	1134	138.59	1127	171.0186	ν CC(13)+b HCC(14)+νOC (15)
1082	1082	1088	20.74	1083	23.313	ν CC(15)
1065		1067	56.74	1060	67.2215	ν CC(11)+b HCC(11)+t HCCC(22)
		1051	28.68	1045	55.3325	t HCCC(12)
		1041	7.89	1037	2.0621	ν CC(25)
1039	1040	1039	2.74	1036	11.3595	νOC(13)+ b CCC(26)+t HCCC(14)
		1015	3.77	1012	2.8419	t HCCC(44)
991	992	986	12.22	982	11.3564	ν CC(40)
960		963	0.5	968	0.3175	t HCCC(53)+t CCCC(13)
		941	0.66	952	0.3506	t HCCN(10)+ t HCCC(81)
		936	0.9	946	0.7508	t HCCC(63)+tCCCC(14)
890	920	914	1.9	909	1.8558	b HCC(11)+tHCCC(31)
854	854	882	0.41	886	0.1214	t HCCC(81)

846		847	1.84	846	2.0975	ν CC(16)+ν NC(10)+t HCCC(10)
		832	3.74	831	3.7893	t HCCN(54)+tHCCC(24)
816	808	798	2.45	798	2.5346	ν CC(13)+t HCCC(12)+NCCC(10)
		785	3.65	784	1.8989	t HCCN(14)+ φOCOC(59)+ φCCCC(13)
777	773	772	7.89	780	8.1691	ν CC(12)
754	743	758	34.39	754	49.9041	ν CC(12)+b CCC(19)+t HCCC(13)
		738	64.89	739	67.7778	t HCCC(19)
		723	2.23	720	1.3944	t HCCC(710
	702	698	21.73	697	36.6822	ν OC (12)+t CCCC(14)
		694	14.76	694	4.0812	t CCCC(68)+ φ OCOC(13)
663		650	59.75	636	51.6726	t CCCC(10)
624	623	625	56.08	621	55.4206	b OCO(69)
		607	9.22	606	9.6515	b CCC(47)+b OCOC(15)
584	577	572	79.97	567	0.4581	t HOCC(76)
550		568	1.05	558	84.7209	b CCC(16)
534		539	4.13	535	4.0303	t CCCN(13)+t CCCC(15)
520		516	8.21	516	9.3742	t CCCC(11)+ φ CCCC(13)
	521	513	10.08	512	10.8472	t CCCC(23)+ φ CCCC(25)
504	505	499	2.36	501	2.0465	ν CC(15)+ b HCC(12)+b CCC(25)
	475	486	5.74	484	6.0456	b NCC(32)+b CCC(23)
474		460	0.28	462	0.1082	b NCC(32)+b CCC(37)
	429	418	6.86	420	8.9128	t HNCC(68)+tCCCC(25)+ φCCCC(13)
		394	3.67	391	4.121	ν NC(11)+b OCC(12)
		346	1.6	345	1.2821	t HNCC(68)
	320	316	1.01	317	1.1985	b NCC(29)+b CCC(37)
	283	291	2.85	290	2.9539	b CCC(66)
		267	4.29	268	6.1751	φ CCCC(47)
	247	241	2.15	237	2.2297	b OCC(44)+b CCC(28)
	215	216	2.69	214	3.2118	t HCCC(14)+t CCCC(30)+ φCCCC(17)
		185	0.67	181	0.9076	t CCCN(38)+ φ CCCC(24)
		167	0.54	165	0.639	t HCCC(44)+ φ CCCC(14)
	152	138	0.32	136	0.3213	b CNC(14)+t CCCC(57)+ φCCCC(10)
	107	131	0.48	129	0.4028	t CCCN(13)+t CCCC(44) + φCCCC(23)
	96	85	0.17	99	0.3088	t HCCC(48)
	84	79	0.19	81	0.1232	b CNC(24)+t CCCC(18)+ φ NCCC(26)+ φ NCCC(26)
		67	0.26	66	0.1645	t CNCC(12)+ OCCC(70)
		33	0.55	36	0.4126	t CCNC(66)+t OCCC(13)
		27	0.95	24	1.0586	t CNCC(71)

ν=Symmetric , b = bending, t = torsion, φ = out of plane bending

$$V(r) = \Sigma \frac{Z_A}{R_A - r} + \int \frac{\rho(r')dr}{|r' - r|}$$

molecular reactive behavior. The electrostatic potential is a powerful tool which provides insights into Intermolecular association and molecular properties of small molecules, actions of drug molecules under analogs [25].The biological function of hemoglobin and enzymecatalysis Electrostatic potential maps illustrates the charge distribution of molecules three dimensionally. The maps enable us to visualize the charge related properties of Molecules [26].Negative electrostatic potential corresponds to attraction of the proton by the concentrated electron density in the molecules (from lone pairs, pi – bond, etc.).Positive electrostatic potential correspond to repulsion of proton by the atomic nuclei in regions where low electron density exists and nuclear charges is incompletely shielded Molecular Electrostatic Potential surface of MFA is shown in Fig.5 represents molecular electrostatic potential surface of MFA.MEP is the physical property that can be determined experimentally by diffraction and by computational methods [27]. The MEP at point r in the space around a molecule in (a.u.) can be expressed as Where Z_A is the charge on nucleus A, located at R_A and $\rho(r')$ is the electronic density function of the molecule. The first and second terms represent the contribution to the potential due to nuclei and electrons respectively. V(r) is the resultant at each point r, which is the net electrostatic effect produced at the point r by both electrons and nuclei of the molecule. The different values of electrostatic potential at the surface are represented by different colours. The potential increases in the order red < orange < yellow < green < blue. Electrophilic regions are represented by red and yellow, nucleophilic by blue and green indicates neutral electrostatic potential. The atoms O8, O9 are electrophilic reacting sites. Nitrogen atom N10 was a nucleophilic site. From these results, the nitrogenatom indicate strongest attraction, while oxygen

atoms indicate strongest repulsion. The figures confirm the different positive and negative sites of the molecule in accordance with the total electron density surface.

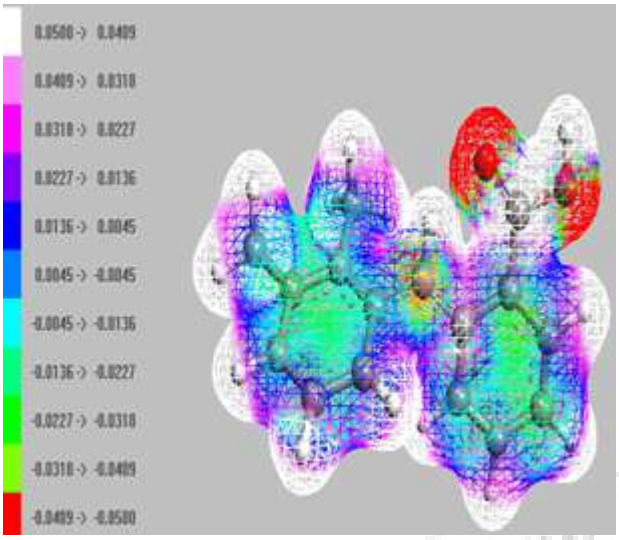

Figure 5: The molecular electrostatic potential surface of MFA

4.5 UV- Visible Spectral analysis

The time dependent density functional method (TD-DFT) is to detect exact absorption wavelengths at a relatively small computing time which correspond to vertical electronic transitions computed on the ground state geometry [28, 29].UV spectral studies are very useful in determining the transmittance and absorption on an optically active material [30].Fig. 6. Shows the UV spectrum of MFA and Table 3 shows the experimental and calculated absorption wavelength (λ), excitation state, Oscillator strength (f), electronic absorption value and transition of MFA. According to Franck-Condon principle, the maximum absorption peak (λ_{max}) corresponds to vertical excitation. Theoretical calculations predicts one intense electronic transition at 441.02 nm with an oscillator strength f = 0.0254 and electronic absorption value 3.0221 ev, which is in good agreement with the experimental value 477 nm, corresponding to HOMO ↔LUMO transition. The observed wavelength 477nm corresponds to n-σ* transition. Another peak at 319.21 nm with an oscillator strength 0.0015 and electronic absorption value 3.8841 eV corresponds to the second excited state with transitions value HOMO ↔LUMO+1, HOMO ↔LUMO+2 . The third peak at 313.47 nm withan oscillator strength 0.0410 and electronic absorption value 3.9552 eV corresponds to the third excited state with transitions value HOMO LUMO+1, HOMO ↔LUMO+2.

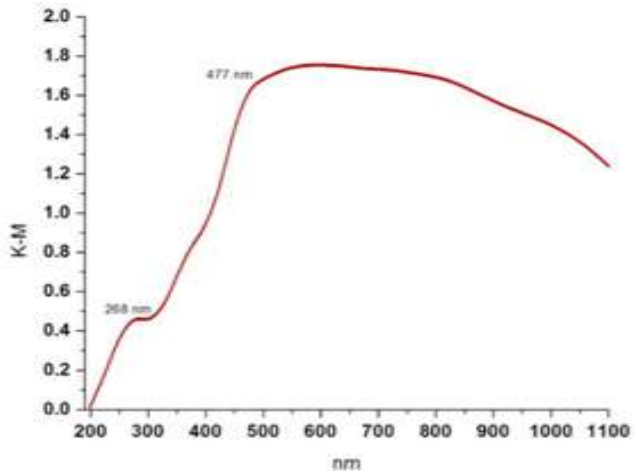

Figure 6: UV spectrum of MFA

4.6 Thermodynamic Properties

Thermodynamic properties like zero point energy, rotational constants, rotational temperatures, molar capacities, energy and entropy of MFA have been calculated using B3LYP/6-311++G(d, p) is shown in the Table 4. The thermodynamic data provide helpful information for further study on MFA. They can be used to compute other thermodynamic energies based on the thermodynamic functions [31]. The statistical thermochemical analysis of MFA was performed considering the molecule to be at room temperature 298.15K and 1 atm pr. The difference in values calculated by both B3 LYP and RHF methods are less. The zero point vibrational energy calculated by B3LYP methods is much lower than by the RHF method. The thermodynamic functions increase with increase in temperature ranging from 100 to 1000K are listed in the Table 5.From this table it is evident that the properties increases with increase in temperature due to the fact that the molecular vibrational intensities increase with temperature .The correlation for this thermodynamic properties are 0.99999, 0.99943, and 0.99949 respectively. The corresponding fitting equations are as follows and the correlation graphs are shown in Fig 7.

$S = 247.8366 + 1.05488T - 2.2397 \times 10^{-4} T^2$ ($R^2 = 0.99999$)
$CP = 7.28273 + 1.0238T - 4.21292 \times 10^{-4} T^2$ ($R^2 = 0.99943$)
$\Delta H = -11.25731 + 0.11338T + 2.8199 \times 10^{-4} T^2$ ($R^2 = 0.99949$)

Table 3: Experimental and calculated absorption wavelength (λ), excitation state, oscillator strength (f), electronic absorption value (eV) and transition of MFA by TD-DFT method (B3LYP/6-311++G (d, p))

Excitation	Singlet A	cal. Wave length (nm)	Wavelength (nm)	oscillator strength (f)	Electronic absorption(ev)	Transition
Excited State 1						
64 > 65	0.6993	477	441 .025	0.0254	3.0221	HOMO ↔ LUMO+1
Excited State 2 63 > 65	0.69363		319.21	0.0015	3.8841	HOMO ↔ LUMO+1
64 > 66						HOMO ↔ LUMO+2
Excited State 3						
63>65	-0.12693		313.47	0.0410	3.9552	HOMO ↔ LUMO+1
64>66	0.68112					HOMO ↔ LUMO+2

Thermodynamic Properties

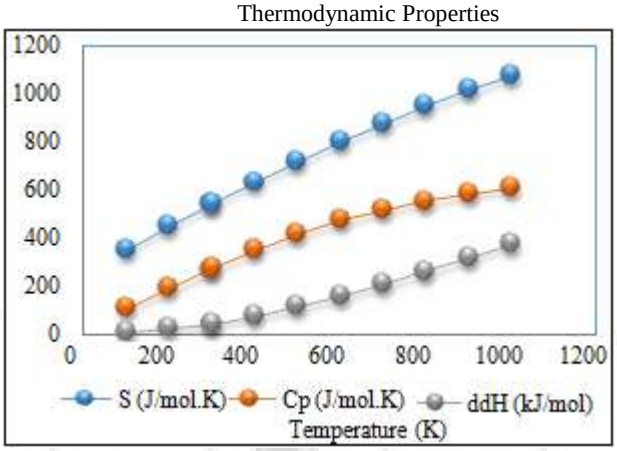

Figure 7: Thermodynamic properties of Mefenamic acid

Table 4: The calculated Thermodynamic Parameters of MFA

Parameters	**B3LYP/6-31G(d, p)**	**B3LYP /6-31++G(d, p)**	RHf Method
Zero point energy(Kcal/Mol)	168.98128	168.54058	179.42878
Rotational constants(GHz)	0.78468	0.78453	0.79695
	0.24891	0.24664	0.24455
	0.20537	0.20694	0.22447
Rotational temperatures (Kelvin)	0.03825	0.03765	0.03825
	0.01174	0.01184	0.01174
	0.01077	0.00993	0.01077
Entropy(CV)			
Total	62.605	62.774	58.989
Translational	2.981	2.981	2.981
Rotational	2.981	2.981	2.981
Vibrational	56.643	56.813	53.027
Specific heat capacity(cal/mol K)			
Total	129.565	129.548	129.07
Translational	42.341	42.341	42.341
Rotational	33.349	33.351	33.263
Vibrational	53.874	53.856	53.466
Energy(Kcal/Mol)			
Total	179.083	178.657	189.125
Translational	0.889	0.889	0.889
Rotational	0.889	0.889	0.889
Vibrational	177.306	176.879	187.347

Table 5: Thermodynamic properties at different temperatures for the MFA B3LYP/6-311++G (d, p)

T (K)	S (J/mol.K)	Cp (J/mol.K)	ddH (kJ/mol)
100	350.52	112.12	7.24
200	451.39	189.26	22.23
298.15	542.14	270.96	44.8
300	543.82	272.5	45.31
400	633.24	351.35	76.58
500	719.1	418.6	115.18
600	800.44	473.43	159.88
700	876.88	517.97	209.53
800	948.51	554.6	263.21
900	1015.65	585.14	320.24
1000	1078.68	610.92	380.08

4.7 Mulliken Population analysis

Mulliken atomic charge analysis plays an important role in the application of theoretical calculation to molecular system, as atomic charges affect properties of molecular systems[32].The electronic charge on an atom determines the bonding capability and molecular conformation. The atomic charge values obtained by the Mulliken population `analysis [33]. Mulliken population analysis was performed on the title molecule by B3LYP and RHF method using 6-31, 6-31++ and 6-311 basis sets and presented in the table 6.The oxygen atoms O8, O9 have charges -0.46471, -0.49678 & -0.436478, -0.436115 in B3LYP and -0.48142, -0.55938 in RHF respectively. The atom N10 has the highest negative value of -0.67287.C1 has maximum positive charge of 0.551513 by B3LYP and 0.73956 by RHF method. All the hydrogen atoms are positive charges and except C1, C2, C3, C4, C11, C12, C13 all the carbon atoms are negative charges .The net charge of hydrogen atom is 1.95262.The presence of negative charge on nitrogen and oxygen atoms and net positive charge on hydrogen atoms may suggest the formation of intermolecular interaction in solid forms [34].The advantage of this population analysis is that it is useful for comparing changes in partial charge assignment between two different geometries with the same basis set. The mulliken charges obtained by B3LYP/6-31/G(d, p), 6-31++/G(d, p) & RHF/6-311G(d, p) methods are shown in the Table 6. The plot of Mulliken charges obtained by three methods are shown in Fig. 6

4.8 Chemical Reactivity

4.8.1 Global reactivity description

Conceptual DFT based descriptors help to understand structure of molecules and their reactivity. Various reactivity descriptors such as electrophilicity, chemical potential, global hardness have been calculated using the energies of the frontier orbital from Koopmans theorem [35] and are given below:

$$I = - E_{HOMO} \text{ and } A = -E_{LUMO}$$

The higher HOMO energy correspond to the more reactive molecule in the reactions with electrophiles, while lower LUMO energy is essential for molecular reactions with nucleophiles [36].Knowing the HOMO-LUMO energy gap, the nature of the molecule (hard or soft) can be determined.

The molecule having a large energy gap are known as hard molecules [37] and those with less energy gap are known as soft molecules. The soft molecules are more polarizable than the

$$\omega = \mu^2/2\eta$$

A good, more reactive, nucleophile is characterized by a lower value ofμ, ω and conversely a good electrophile is characterized by a high value of μandω. Table 7 presents the value of electronegativity (χ), chemical potential (μ), global hardness (η), global Softness(S) and global electrophilicity index (ω).

4.8.2 Local reactivity descriptors

Fukui function is used to model chemical reactivity and site selectivity [40].Fukui function (f_k^+, f_k^-, f_k°,) local softness (S_k^+, S_k^-, S_k°) and local electrophilicity indices (ω_k^+, ω_k^-, ω_k°) of MFA have been listed in table 7.Using Hirshfield atomic charges of neutral, cation and anion states of MFA, Fukui function is calculated using the following relations.

f_k^+ = [q(N+1)-q(N)] for nucleophilic
f_k^- = [q(N)- q(N-1)] for electrophilic
f_k° = [q (N+1)-q (N-1)] for radical attack

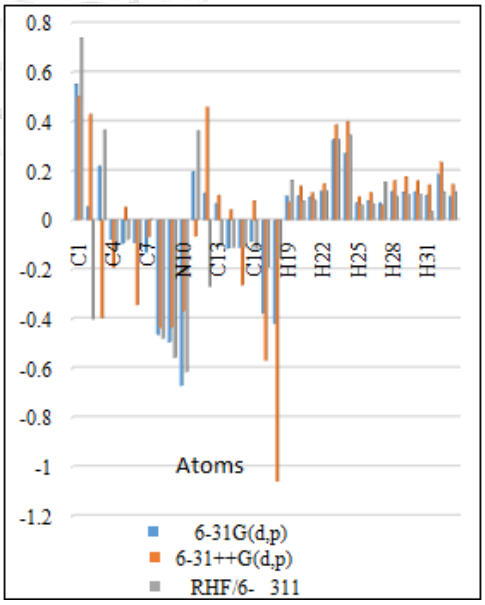

Figure 8: Plot of Mulliken charges obtained by by B3LYP/6-31/G(d, p) 6-31++G(d, p), RHF/6-311G(d, p)

Atom	B3LYP/6-31G(d, p)	B3LYP/ 6-31++G(d, p)	RHF/6-311G(d, p)
C1	0.551513	0.500375	0.73956
C2	0.053957	0.429088	-0.40296
C3	0.218771	-0.396986	0.365119
C4	-0.07856	-0.192403	-0.1213
C5	-0.09575	0.053055	-0.08017
C6	-0.09259	-0.344365	-0.11838
C7	-0.13082	-0.068345	0.003827
O8	-0.46471	-0.436478	-0.48142
O9	-0.49678	-0.436115	-0.55938
N10	-0.67287	-0.37008	-0.61728
C11	0.195963	-0.06741	0.361455
C12	0.108044	0.458109	-0.26954
C13	0.068236	0.101055	-0.10357
C14	-0.11585	0.042063	-0.11213
C15	-0.11118	-0.264333	-0.11002
C16	-0.08824	0.078567	-0.11634
C17	-0.3794	-0.569373	-0.1895
C18	-0.42235	-1.059904	-0.15511
H19	0.098331	0.073794	0.161493
H20	0.099435	0.137204	0.079314
H21	0.093825	0.11135	0.082308
H22	0.116066	0.14893	0.118412
H23	0.327049	0.385817	0.327313
H24	0.271019	0.399727	0.344679
H25	0.07201	0.094288	0.061137
H26	0.078543	0.112171	0.066403
H27	0.069056	0.060598	0.155535
H28	0.115346	0.160547	0.096215
H29	0.112437	0.175874	0.104751
H30	0.115598	0.160907	0.104768
H31	0.100939	0.142385	0.035214
H32	0.186658	0.235673	0.114784
H33	0.096308	0.144213	0.114793

Table6: The Mulliken charges obtained by B3LYP/6-31G (d, p), 6-1++G(d, p)& RHF/6-311G (d, p)

require less energy for excitation. The hardness of the molecule is determined by the formula

$\eta = 1/2(I-A)$

$\eta = \frac{1}{2}(E_{LUMO} - E_{HOMO})$

And global softness inverse of global hardness is obtained by the formula

$S = \frac{1}{2}\eta$

The electron affinity can also be used in combination with ionization energy to give electronic chemical potential (μ) defined by Parr and Pearson [38] as the characteristic of electronegativity of molecules.

$\mu = -1/2\ (I+A)$

$\mu = -\chi = \frac{1}{2}(E_{LUMO}+E_{HOMO})$

$\mu = -\chi$

$\chi = -\frac{1}{2}(E_{LUMO}+E_{HOMO})$

The global electrophilicity index (ω) was introduced by Parr [39] and calculated using the electronic potentialμ and chemical hardness η

Where N, N-1 and N+1 are total electrons present in neutral, cation and anion state of molecule respectively.f_k^+, f_k^- describe the ability of an atom to accommodate an extra electron or to cope with the loss of an electron and f_k° is consider as an indicator for radical reactivity q_k is the atomic charge at the kth site. Local softness and electrophilicity indices are calculated using the following relations

$S_k = Sf_k^- . S_k = Sf_k^- .S_k^\circ = Sf_k^\circ$

$\omega_k = \omega_k^- . \omega_k = \omega f_k^- .\omega_k^\circ = \omega f_k^\circ$

Where +, - and 0 signs indicate nucleophilic, electrophilic and radical attack respectively. From Table 7, it has been observed that C2 have higher f_k^- value indicating it as possible sites for From the table, the highest nucleophilic attack site was found to be C13 and other sites were C1, C4, C6, C7, C16, H24, H27.Theradialelectrophilic attack .The other sites for Electrophilic attack wereO9, C3, C11, H31, H32is the most preferred site for electrophilic attack was predicted at C2, C11, C12, C13, C14.Of allthe attacks, it was observed that nucleophilic was biggest reactivity site compared to electrophilic and radical attack.

4.9 Conclusion

Thus a complete vibrational band assignment of Mefenamic acid has been carried out using infrared and Raman spectra. The equilibrium geometry computed by DFT level for both the bond lengths and bond angles are performed better. The vibrational frequencies analysis by B3LYP/6-31G (d, p), 6-31++G(d, p) and RHF/6-311++G(d, p) methods agree satisfactorily with experimental results. Several thermodynamic parameters were obtained and analyzed with RHF and DFT methods using the same basis sets.UV spectral analysis of the molecule was also carried out. Mulliken atomic charges of the molecule were studied by both the RHF and B3LYP using the same basis set. The HOMO and LUMO energies show that charge transfer occur within the molecule. Using Mulliken population analysis, Fukui functions, local softness and local electrophilicity indices has been calculated. On the basis of agreement between the calculated and experimental results, assignments of all the fundamental vibrational modes of MFA were examined and proposed.

Table 7: Using Mulliken population analysis, Fukui functions, local softness and local electrophilicity indices in ev for MFA

	q_N	q_{N+1}	q_{N-1}	f_k^+	f_k^-	f_k°	s_k^+	s_k^-	s_k°	w_k^+	w_k^-	w_k°
1 C	*-0.098794*	*0.086631*	*0.108466*	0.185425	-0.20726	-0.0109175	0.0387724	-0.0433381	-0.0022828	0.1031801	-0.1153302	-0.0060751
2 C	*1.026874*	*0.017246*	*-0.027074*	-1.009628	1.053948	0.02216	-0.2111132	0.2203805	0.0046337	-0.5618094	0.5864714	0.012331
3 C	*-0.323066*	*-0.556538*	*-0.552712*	-0.233472	0.229646	-0.001913	-0.048819	0.048019	-0.0004	-0.1299159	0.127787	-0.0010645
4 C	*-0.223682*	*0.151812*	*0.314729*	0.375494	-0.538411	-0.0814585	0.0785158	-0.1125817	-0.017033	0.2089443	-0.2995998	-0.0453277
5 C	*-0.090665*	*-0.240065*	*-0.087255*	-0.1494	-0.00341	-0.076405	-0.0312395	-0.000713	-0.0159763	-0.0831339	-0.0018975	-0.0425157
6 C	*-0.493761*	*-0.309408*	*-0.087255*	0.184353	-0.406506	-0.1110765	0.0385482	-0.0850004	-0.0232261	0.1025836	-0.226201	-0.0618087
7 C	*-0.493416*	*-0.123787*	*0.1024*	0.369629	-0.595816	-0.1130935	0.0772894	-0.1245851	-0.0236479	0.2056808	-0.3315429	-0.0629311
8 O	*-0.3044*	*-0.439997*	*-0.239636*	-0.135597	-0.064764	-0.1001805	-0.0283533	-0.0135422	-0.0209477	-0.0754532	-0.0360381	-0.0557456
9 O	*-0.176982*	*-0.440124*	*-0.400585*	-0.263142	0.223603	-0.0197695	-0.055023	0.0467554	-0.0041338	-0.1464259	0.1244243	-0.0110008
10 N	*0.080362*	*-0.021143*	*0.081891*	-0.101505	-0.001529	-0.051517	-0.0212247	-0.0003197	-0.0107722	-0.0564827	-0.0008508	-0.0286667
11 C	*-0.301934*	*-0.454491*	*-0.582902*	-0.152557	0.280968	0.0642055	-0.0318997	0.0587504	0.0134254	-0.0848906	0.1563452	0.0357273
12 C	*0.655405*	*-0.130336*	*-0.228294*	-0.785741	0.883699	0.048979	-0.1642984	0.1847815	0.0102415	-0.4372271	0.491736	0.0272545
13 C	*0.004222*	*0.922154*	*0.871437*	0.917932	-0.867215	0.0253585	0.1919396	-0.1813347	0.0053025	0.510785	-0.4825634	0.0141108
14 C	*-0.294486*	*-0.746553*	*-0.767254*	-0.452067	0.472768	0.0103505	-0.0945272	0.0988558	0.0021643	-0.2515535	0.2630727	0.0057596
15 C	*-0.302498*	*-0.277664*	*-0.232769*	0.024834	-0.069729	-0.0224475	0.0051928	-0.0145803	-0.0046938	0.0138189	-0.0388008	-0.012491
16 C	*-0.044555*	*0.429342*	*0.653705*	0.473897	-0.69826	-0.1121815	0.0990919	-0.1460062	-0.0234572	0.2637009	-0.3885481	-0.0624236
17 C	*-0.460564*	*-0.482326*	*-0.388892*	-0.021762	-0.071672	-0.046717	-0.0045504	-0.0149866	-0.0097685	-0.0121095	-0.039882	-0.0259958
18 C	*-0.870545*	*-0.820808*	*-0.729665*	0.049737	-0.14088	-0.0455715	0.0104	-0.029458	-0.009529	0.0276762	-0.0783929	- 0.0253583
19 H	*0.106736*	*0.065749*	*0.102802*	-040987	003934	-0185265	-.0085704	0.0008226	-.0038739	-.0228073	0.002189	-.0103091
20 H	*0.190279*	*0.063277*	*0.211454*	-0.127002	-0.021175	-0.0740885	-0.0265561	-0.0044277	-0.0154919	-0.0706705	-0.0117829	-0.0412267
21 H	*0.166897*	*0.074573*	*0.211286*	-0.092324	-0.044389	-0.0683565	-0.0193049	-0.0092817	-0.0142933	-0.0513739	-0.0247003	-0.0380371
22 H	*0.208125*	*0.157884*	*0.249141*	-0.050241	-0.041016	-0.0456285	-0.0105054	-0.0085764	-0.0095409	-0.0279567	-0.0228234	-0.0253901
23 H	*0.290333*	*0.32936*	*0.398957*	0.039027	-0.108624	-0.0347985	0.0081605	-0.0227133	-0.0072764	0.0217166	-0.060444	-0.0193637
24 H	*0.318355*	*0.660004*	*0.689131*	0.341649	-0.370776	-0.0145635	0.0714388	-0.0775293	-0.0030452	0.1901112	-0.206319	-0.0081039
25 H	*0.151364*	*0.038483*	*0.156195*	-0.112881	-0.004831	-0.058856	-0.0236034	-0.0010102	-0.0123068	-0.0628128	-0.0026882	-0.0327505
26 H	*0.168127*	*0.093222*	*0.207251*	-0.074905	-0.039124	-0.0570145	-0.0156626	-0.0081808	-0.0119217	-0.041681	-0.0217706	-0.0317258
27 H	*0.090902*	*0.302634*	*0.304444*	0.211732	-0.213542	-0.000905	0.0442732	-0.0446516	-0.0001892	0.1178187	-0.1188259	-0.0005035
28 H	*0.15374*	*0.142858*	*0.181161*	-0.010882	-0.027421	-0.0191515	-0.0022754	-0.0057337	-0.0040046	-0.0060553	-0.0152585	-0.0106569
29 H	*0.166561*	*0.120801*	*0.172076*	-0.04576	-0.005515	-0.0256375	-0.0095684	-0.0011532	-0.0053608	-0.0254632	-0.0030688	-0.014266
30 H	*0.156501*	*0.120736*	*0.172054*	-0.035765	-0.015553	-0.025659	-0.0074785	-0.0032521	-0.0053653	-0.0199015	-0.0086545	-0.014278
31 H	*0.161393*	*0.001598*	*-0.009858*	-0.159795	0.171251	0.005728	-0.0334131	0.0358086	0.0011977	-0.0889182	0.0952929	0.0031874
32 H	*0.240563*	*0.132475*	*0.194554*	-0.108088	0.046009	-0.0310395	-0.0226012	0.0096205	-0.0064904	-0.0601458	0.0256018	-0.017272
33 H	*0.14261*	*0.132404*	*0.194361*	-0.010206	-0.051751	-0.0309785	-0.0021341	-0.0108211	-0.0064776	-0.0056791	-0.0287969	-0.017238

5. Acknowledgement

The author is very much thankful to Sophisticated Analytical Instrumentation facility (SAIF-SPU), Research Lab St. Peter's University, Avadi, Chennai-600054 for providing the facilities for FTIR-ATR and UV-Visible spectrum for the entire research and Sophisticated Analysis Instrument Facility, Indian Institute of Technology, Madras, India, for providing the facilities for spectral measurements. The author is also thankful to Management MSEC to show a keen interest in this work and also thankful to Secretary Ln.Dr.Ms.K.S.Lakshmi and our Principal Dr.K.S.Ms.Babai for using the Research lab in Meenakshi women's College, Kodambakkam, and Chennai.

References

[1] Jilani, J. A., Pillai, G. K., Salem, M. S., & Najib, N. M.Jornal Drug evelopment and Industrial Pharmacy vol 23, (1997)., 319-323.
[2] Vinit D.Patil, Vineyak J.Kadam, Santosh N.Shinde, Anirudddha R.Chabukswar, Swati C, Jagdale, Bhanudas S, Kuchekar Der paharmacia letter 2010, 2(3): 304-308.
[3] Makoto et al., Journal of pharmaceutical Sciences, Vol.99, 4048-4053, No.9.Sep 2010.
[4] Siti kholijah Abdul Mudalip, MOhd, Rushdi Abu Bakar, Fatmawati Adam, and parveen Jamal., International Journal of chemical Engineering and Applications, Vol.4, No.3, June 2013.
[5] Lian Fang, Sachihiko Numajiri, Daisuke kobayashi, Hideo veda, Koji Nakayama, Journal of Pharmaceutical Sciences Jan 93, issue 144- 154.
[6] Umang V.Shah, Dolapo olusanmi, Ajits NArang, Munir A, Hussain, John F.Gamble, Michael J.Tobyn, Jerry .Y.Y.Heng., International Journal of Pharmaceutics, Vol.472, sep 2014, 140-147.
[7] Serapcesur, cihan yaylaci journal of crystallization process and Technology;vol.2 NO.3 (2012), Article ID: 21356.
[8] Vanessa R.R.cunha. cells M.S.Izumi, philippe A, D.petersen, Alvicle'er Mayihaae, Marcia L.A.Temperini, Helena M.Petrilli and Vera R.L.contantino, Journal of physical chemistry B.Vol 118. Mar 24, 2014.
[9] Mudit Dixitad partha sarathi K Kulkarani., Elixir Biophys.39 (2011) 5026-5029.
[10] M. J. Frisch, G. W. Trucks, H. B. Schlegel, G. E. Scuseria, M. A. Robb, J. R. Cheeseman, G. Scalmani, V. Barone, B. Mennucci, G. A. Petersson H. Nakatsuji, M. Caricato, X. Li, H. P. Hratchian, A. F. Izmaylov, J. Bloino, G. Zheng, J. L. Sonnenberg, M. Hada, M. Ehara, K. Toyota, R. Fukuda, J. Hasegawa, M. Ishida,

T. Nakajima, Y. Honda, O. Kitao, H. Nakai, T.Vreven, J. A. Montgomery, Jr., J. E. Peralta, F. Ogliaro, M. Bearpark, J. J. Heyd, E. Brothers, K. N. Kudin, V. N. Staroverov, T. Keith, R. Kobayashi, J. Normand, K. Raghavachari, A. Rendell, J. C. Burant, S. S. Iyengar, J. Tomasi, M. Cossi, N. Rega, J. M. Millam, M. Klene, J. E. Knox, J. B. Cross, V. Bakken, C. Adamo, J. Jaramillo, R. Gomperts, R. E. Stratmann, O. Yazyev, A. J. Austin, R. Cammi, C. Pomelli, J. W. Ochterski, R. L. Martin, K. Morokuma, V. G. Zakrzewski, G. Voth, P. Salvador, J. J. Dannenberg, S. Dapprich, A. D. Daniels, O. Farkas, J. B. Foresman, J. V. Ortiz, J. Cioslowski, and D. J. Fox, Gaussian Inc., Wallingford CT, 2013.

[11] H.B.Schlegel, J.Comput.chem.3 (1982) 214-218.

[12] A.D.Becke, Phys, Rev.A 38 (1988) 3098-3100.

[13] C.Lee, W.Yang, R.G.Parr, Phys.Rev.B 37 (1988) 785-789.

[14] B.G.Johnson, M.J.Frisch, chem. Phys.Lett.216 (1993) 133-140.

[15] W.J. Hehre, L.Random, P.V.R. Schleyer, A.J. Pople, Ab Initio Molecular Orbital Theroy, Wiley, New York, 1989.

[16] David Ortegon-Reyna, Cesar Garcias-Morales, Efren V.Garcia-Baez, Armando Ariza-Castolo and Franscisco J. Martinez- Martinez.Ortegon- Reyna et al. 020757]

[17] S.Gunasekaran, R.K.Natarajan, D.Syamala, R.Rathika, Ind. J. Pure Apple. Phys. 44 (2006)315

[18] D.Sajan, I.HubertJoe, V.S.Jyakumar, J.Zaleski, J.Mol.Structure .785(2006) 43-53

[19] B.Smith, Infrared Spectra Interpretation;A Systematic ApproCH, CRC, Washington, DC, 1999.

[20] N.P.G.Roges, A.Guide to the Complete Interpretation of infrared Spectra of Organic Structure, Wiley, New York, 1994.

[21] M.Arivazhagan, D.Anitha, Spectrochim, Acta Part A 104(2013) 451-460.

[22] G Varanyi, assignments for vibrational spectra of seven hundred Benzene derivatives, Vol I -2, Academic Kiaclo, Budapet 1973.

[23] M Arivazhagan, D Amitha Rexalin, Spectrochim Acta A 83 (2011) 553-560.

[24] G.R. Ramkumar, S.Srinivasan, T.J Bhoopathy, S.Gunasekaran Spectrochim, Acta A 99(2012) 189-195.

[25] Gunasekaran S, Balaji R A Kumerasan S, Anand G & Srinivasan S, Can J Anal Sci Spectrosc, 53(2008) 149.

[26] H.Weinstein, S.Maayani, K.S.Srebreni, S.S. Cohen, M.Sokolvosky.Mol.Pharmorol.11 (1975)671-689.

[27] C.Munoz-Caro, A.Nino, M.L.Semenr, J.M.Leal, S.Lbeans.J.Org.Chem.65 (2000), 405-410.

[28] Whiffen DH&Thompson H W, J Chem Soc, 263(1945)1350.

[29] D.Jacquemin. J.Preat, E.A. Perpete, Chem Phys Lett. 40(2005) 254-259.

[30] M.Cossi, V. Barone, J.Chem.Phys.115 (2001) 4708-1717.

[31] C.N.R. Rao, Ultraviolet and Visible Spectroscopy Chemical Applications Plenum Press, New York 1975.

[32] Tzeng W B, Narayan K, Lin J L & Tung C C, Spectrochim, A55 (1999) 153.

[33] V.K.Rastogi, M.A.Palatox, L. Mittal, N.Peica, W.Kiefer, K.Lang, P.Ohja, J.Raman Spectrosc, 38(2007) 1227-1241.

[34] R.S.Mulliken, J.Chem.Phys.23 (1955) 1833-1840.

[35] Xiao-Hong et al., Theor.Chem.969 (2011) 27-34.

[36] T.Koopmans, Physica 1 (1933) 104-113.

[37] A.Rauk, Orbital Interaction Theory of Organic Chemistry, Second ed, . John Wiley & Sons, New York, 2001.

[38] R.G. Pearson, J.Am.Chem, Soc.107 (1985) 6801-6806.

[39] R.G.Parr, R.G.Pearson, J.Am.Chem.Soc. 105(1983) 7512- 7516.

[40] R.G.Parr, L.Szentpaly, S.Liu, J.Am.Chem.Soc.121 (1999) 1922-1924.